Mine Water and the Environment (2022) 41:629–639
https://doi.org/10.1007/s10230-022-00852-z

TECHNICAL ARTICLE

Experimental Investigation on the Transport Behavior of a Sand/Mud/Water Mixture Through a Mining-Induced Caving Zone

Yankun Liang[1,2] · Wanghua Sui[2] · Tong Jiang[1,3] · Xiangyang Shen[1,3]

Received: 15 August 2021 / Accepted: 14 February 2022 / Published online: 8 March 2022

Abstract

The transport of sand particles through various mining-induced caving zones was investigated experimentally under different initial infiltration water heads. These experiments were performed in a laboratory-scale caving zone packed with glass beads, using four different sizes of sand grains. The transports were categorized into two different patterns: seepage and driven. The probability of the driven pattern was greatly increased by increasing the height of the initial water head and the size ratio R_s (the ratio of glass beads to sand particles by diameter). The sand portion of the sand/mud/water mixture had a high transport rate while the water had a low one in the mixture. Both rates increased with increasing initial water head height, with a larger increase in the sand transport rate than the water flow rate. The water flow rate is primarily governed by the permeability of the sand layer, while the sand transport rate is greatly affected by R_s. These findings provide an insight into the mechanism of sand/mud/water mixture inrushes and a potential design idea for its control and treatment.

Keywords Inrush · Transport pattern · Initial water head · Sand transport rate · Water flow rate

Introduction

The inrush of water along with large volumes of sand into tunnels or panels is a major geohazard in many of China's underground mines (Chen et al. 2014; Miao et al. 2010; Qian 2012; Sui et al. 2008; Xue et al. 2021). Statistics show that since the 2000s, more than 80 geohazards in underground mining have involved water and sand mixture inrushes in western China, causing serious financial losses and even casualties (Qian et al. 2019; Zhao et al. 2013). For example, the Halagou coal mine was subjected to an extremely large water and sand mixture inrush on 28 July 2009. Within 5 h, the maximum height of the sand had reached the top of the face belt conveyor, and a funnel-shaped collapse with a diameter of 47 m and a depth of 12 m formed on the ground surface. In 2011, a water and sand mixture inrush disaster occurred at the Buertai coal mine in the Inner Mongolia Autonomous Region (Zhang et al. 2015). This inrush buried 60 hydraulic supports at the panel and led to the formation of a 50 m diameter collapse pit at the surface. Mining production was interrupted for 16 days, which resulted in a direct financial loss of ≈ 70 million CNY. On 7th April 2016, the Zhaojin coal mine had a large water and sand mixture inrush, which left 11 casualties and large financial losses. Recently, a large-scale water and sand mixture inrush in the Haojialiang coal mine was reported on 15th July 2021, resulting in 5 casualties and great financial losses (China Central Television 2021).

Water and sand mixture inrush hazards most commonly occur as the underground panel approaches or passes through weak geological strata with fissures and faults, as well as mining-induced fractured zones or caving zones (Butcher et al. 2005; Chen et al. 2021; Dong et al. 2020; Sui et al. 2011). Fractures are generally considered to be the main geological pathways that trigger water and sand mixture inrush hazards and have received considerable attention (Cochard and Ancey 2009; Haza et al. 2013; Li

✉ Wanghua Sui
suiwanghua@cumt.edu.cn

1 Henan Province Key Laboratory of Rock and Soil Mechanics and Structural Engineering, North China University of Water Resources and Electric Power, Zhengzhou, China

2 School of Resources and Geosciences, Institute of Mine Water Hazards Prevention and Controlling Technology, China University of Mining and Technology, Xuzhou, Jiangsu, China

3 College of Geosciences and Engineering, North China University of Water Resources and Electric Power, Zhengzhou, China

et al. 2016; Liu and Li 2016; Sui et al. 2007; Yang et al. 2019b). Recently, increasing attention has been paid to mining-induced caving zones, which serves as a pathway for water and sand between the mining panel and overlying unconsolidated aquifers (Du et al. 2018a; Liang et al. 2017). For example, subsequent investigations after the Haojialiang coal mine water and sand inrush found that the height of the caving zone was greatly increased by the thin bedrock and high-intensity mining activities, which resulted in the caving zone reaching an unconsolidated sand layer and the water inside it (Dept. of Emergency Management of Shaanxi Province 2021).

Due to the uncertainties and invisibility of the actual geological conditions in coal mines, it is difficult to study the water and sand mixture inrush mechanism by using in situ observations and tests. In addition, as sand particle flow has strong randomicity, the application of numerical simulation and theoretical analysis methods has some restrictions. Therefore, well-controlled laboratory testing is a good way to study the conditions and mechanism of water and sand mixture inrush (Du et al. 2018b; Guo et al. 2016; Sui et al. 2007). Chen et al. (2016) examined the water sand seepage characteristics of broken rock using a modified Material Test System (MTS816), and showed that there is a substantial increase in sand filtering with an increased hydraulic gradient and initial porosity, but deformation experience has no significant influence on the water seepage characteristics. This agrees well, qualitatively, with the findings of Du et al. (2017), who conducted flow experiments using a modified testing system. Furthermore, Zhang et al. (2021) used a developed seepage test system to study the flow behavior of water and sand mixtures in fractured rock specimens. The outflow of aeolian sand was found to be affected by the particle size distribution, void ratio, and initial mass of aeolian sand. Yang et al. (2019a) further studied the effects of the particle-size distribution on the seepage behavior of sand-particle mixtures subjected to a high hydraulic gradient, and identified three different flow regimes: a Darcy regime, a Forchheimer, and a turbulent regime. These studies were conducted using a modified seepage test system; the solid concentration of the mixtures was less than 20%, and sand/mud/water mixtures were generally considered a single-phase flow. However, sand/mud/water mixture inrushes usually contain large volumes of sand with a high solid content, which can be regarded as dense rapid flow (Forterre and Pouliquen 2008; Miao et al. 2010; Sui et al. 2011), and the flow behavior of dense rapid flow is quite different from that of a dilute flow with a low solid content (Campbell 2006; Chen and Yu 2015; Goldhirsch 2003; Yang et al. 2020). There is evidently a lack of research on the transport behavior of high solid concentrations through caving zones, which was the focus of this study.

In this work, an independent developed test system was used to visually observe the mixed flow of a high solids mixture through the caving zone. A series of experiments was performed to examine the transport mechanisms under various experimental conditions. The transport of sand/mud/water mixtures with high solids through porous skeletons was experimentally investigated under different hydrodynamic conditions. The results are helpful for understanding the transport behavior of sand/mud/water mixtures, and provide a potential design concept for remedial measures for sites where sand/mud/water mixture inrush hazards exist.

Materials and Methods

Experimental Setup

The coal mines in western China have three geological characteristics: shallow coal seam depths, relatively thin amounts of overlying bedrock, and a land surface that is mostly covered with aeolian sand. High-intensity and large-scale underground mining in this area can result in the caving zone directly contacting the aeolian sand aquifers, allowing the water and sand in the aquifer to flow into the panels through the caving zone. Figure 1a shows a typical engineering geological model for a water and sand mixture inrush through a caving zone. To study the transport of water and sand mixtures in the caving zone on a laboratory scale, the experimental model was idealized, and the experimental setup was simplified (Fig. 1b).

Figure 1b shows that the transport of a sand/mud/water mixture can be simplified to a cylinder with an internal diameter of 200 mm. The test equipment consists mainly of a water and sand supply system, a caving zone model, and a real-time image acquisition system.

A 1200 mm tall water and sand flow supply system was used mainly to provide a mixed water and sand flow during testing. The control valve was vertically attached between the sand column and the porous skeleton so that the sand and water would flow into the caving zone model when the flow control valve was fully open for the commencement of the testing.

The caving zone is usually modeled by crushed rock masses, steel balls, or glass beads (Du et al. 2017; Sui et al. 2017; Yang et al. 2020; Zhang et al. 2021). In this study, a 350 mm tall caving zone model was packed with glass beads, which is assumed to be the simplest laboratory-scale representation. A wire mesh was placed at each end of the packed column to prevent glass beads from flowing out during the test. The wire mesh spacing was 10 mm and the width of the grid line was 1 mm; the retarding effect of the grid on the overlying water and sand mixture flow can be neglected after repeated testing.

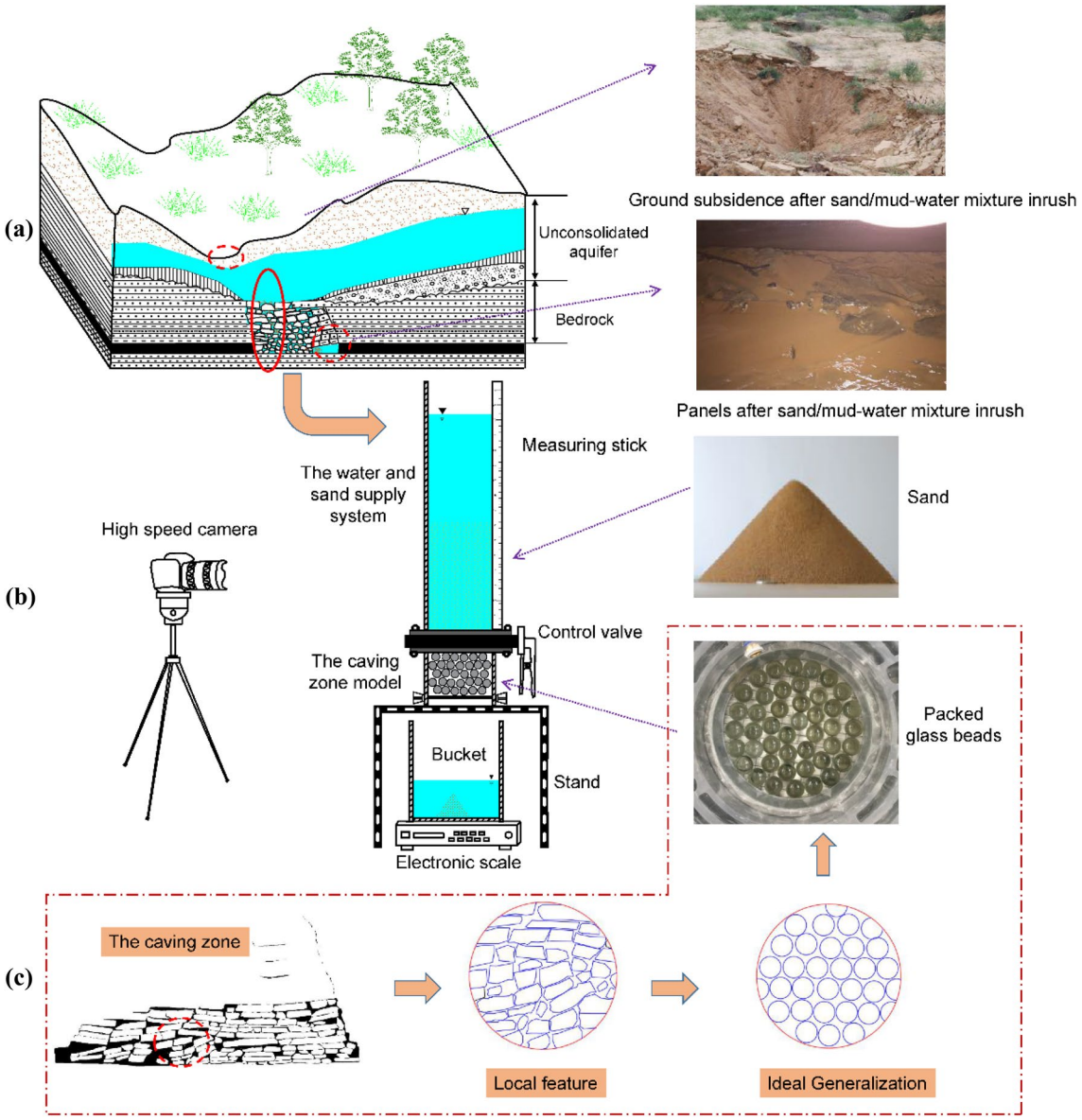

Fig. 1 Schematic diagram of **a** engineering geological model for sand/mud/water mixture inrush through caving zone, **b** experimental setup, and **c** caving zone simplification

A bucket collected the outflow from the porous skeletons; the discharge of sand and water mixture was measured at regular time intervals with a scale until the test was completed. In addition, the propagation of the sand and water flowing through the porous medium was captured using a high-speed camera.

Materials

The grain size distribution curves of the aeolian sand at different depths are shown in supplemental Fig. S-1. The aeolian sand ranges in size from 0.005–2 mm and the clay content is very low. Similarly, the grain size distribution of sand from the coal mines in eastern China that undergo sand/mud/water inrushes shows that the clay content of sand that easily undergoes sand/mud/water mixture inrush is very low. This characteristic is consistent with the conclusion that the possibility of sand/mud/water mixture inrush weakens as the clay content increases (Chen et al. 2021). Therefore, four narrow-screened sand particles without clay were used in this study, with particle sizes (d) of: 0.1–0.25 mm, 0.25–0.5 mm, 0.5–1.0 mm, and 1.0–2.0 mm.

To reduce the possible difficulties associated with a real broken rock mass in the caving zone, the caving zone is usually generalized into a uniform porous medium (Fig. 1c). In this experiment, glass beads were used as the

packing material instead of a real broken rock to eliminate numerous uncertainties that would have considerably complicated analysis of the experimental data. The diameters (D) of the glass beads used were 25, 21, and 16 mm. The data show that the porosity of the caving zone was up to 30%-45% (Zhang et al. 2020). Due to the limited size of the model box, the arrangement of equal-diameter glass beads in the experimental model was between the square and hexagonal arrangements. The porosity of the porous media in this study was ≈ 40–46%.

Experimental Procedure

The porous medium was packed with glass beads before each test. Then, the sand column was built by manually compacting 10 layers of sand particles; the apparent dry density was maintained at 1.57 g/cm^3 and the height of the sand column was set at 500 mm. Subsequently, water was gradually injected into the sand column until the desired water column height (i.e. 500, 600, 700, 800, and 1000 mm) in the tube was reached. After the preparation steps, the flow control valve and electronic scale were opened simultaneously, and sand particles and water flow were filmed using a high-speed camera. After a sufficiently long-time interval with no more sand and water flowing out, the experimental setup was washed to remove any residual sand particles. The experimental procedure was then repeated by repacking the porous medium and sand column from one run to the next. Three repeated tests were performed for each test trial to minimize any possible errors.

Results and Analysis

Transport Patterns

Because of the changes in the height of the top free surface of the sand layer and water head, the dynamics were categorized into two flow patterns. Figure 2 shows pictures of two typical experiments for (D, d) = (21 mm, 0.25–0.5 mm), in which a series of images captured during the flow are presented consecutively. The pattern in Fig. 2a is labeled as a seepage pattern. This transport pattern is normally observed when the H value was relatively low. After the control valve was opened at t = 0 s, sand particles gradually flowed into the porous column due to gravity and hydraulic head pressure, and the height of the water head and sand layer decreased with time. At t = 90 s, the height of the water head was below that of the sand layer. At t = 110 s, the sand in the cylinder column still maintained a certain height after the water had entirely drained out.

When the initial height of the water head was further increased, the transport phenomenon shown in Fig. 2b occurred, which is called the driven pattern. After the start of each test, the sand and water mixture flowed into the porous medium. However, when the top free surface of the sand layer first flowed into the porous medium at t = 50 s, the water head still maintained a certain height.

The corresponding accumulated mass of the sand water mixture and solid concentration vs. time are shown in Fig. 3. The solid concentration generally refers to the mass ratio of sand particles to the sand/mud/water mixture in the water and sand mixture inrush accident (Yang et al. 2018). Note that the overall process of mass accumulation of the mixture and solid concentration evolution during the tests can be divided into three different stages: (1) initial stage, during

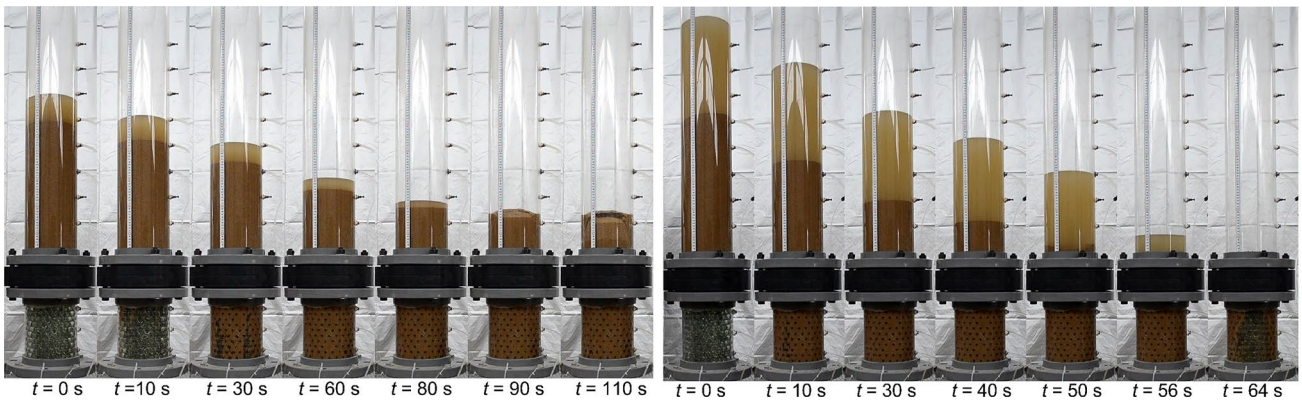

(a) Seepage regime **(b)** Driven regime

Fig. 2 Photos of sand-water mixture flow through the porous medium at different times: **a** seepage regime for (H, D, d) = (600, 21, 0.25–0.5); **b** driven regime for (H, D d) = (900, 21, 0.25–0.5)

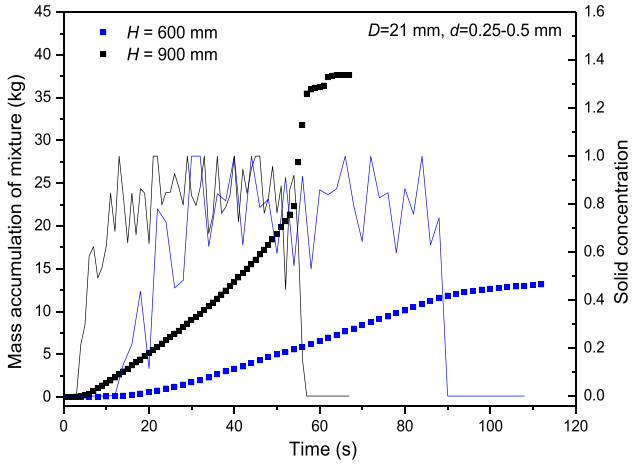

Fig. 3 The mass accumulation of sand-water mixture and solid concentration the time for (D, d) = (21, 0.25–0.5) under different hydraulic conditions

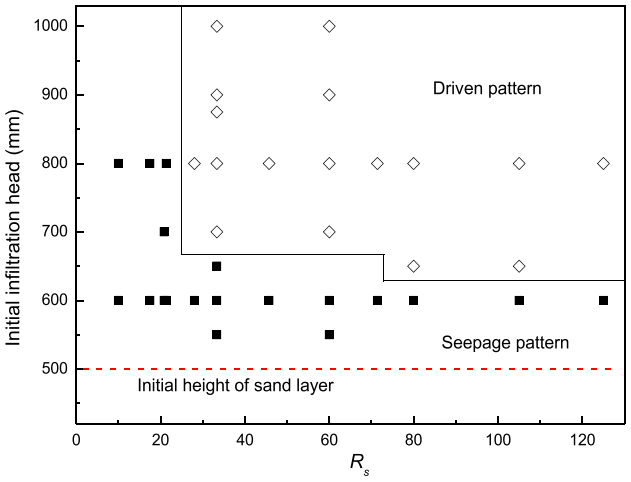

Fig. 4 Boundary between driven and seepage patterns by the size ratio (R_s) and the infiltration heads

which the sand water mixture and solid concentration are almost zero. At this stage, a large portion of the sand-water mixture flows through the porous medium, and only some water in the saturated sand layer first reaches the bucket at this stage. Thus, the sand particle concentration approaches zero. As the sand and water mixture continuously flows from the porous medium, the cumulative mass of the sand-water mixture gradually increases, and the solid concentration of the water–sand mixture increases rapidly in a short time. Then, the sand and water inrush proceeds to the next stage (2), the stabilization stage, during which the solid concentration generally remains constant and shows notable fluctuations. However, the accumulated curves of the discharged mass increase linearly with time, which means that the water/sand mixture per unit time is almost constant. The water and sand inrush amounts fluctuate alternately. In the final stage (3), the solid concentration suddenly decreases to approximately zero, whereas the discharged cumulative mass of the mixture substantially increased in the seepage pattern, while the discharged mass burst to a high value in the driven pattern, because the water column suddenly entered the porous medium a short time after the sand layer was removed from there. Since there was still a sand layer deposited on the porous medium, the total discharged mixture was quite small compared with the discharged mixture in the driven pattern.

Transitions of Transport Patterns

Note that the two transport patterns occured in a certain order, and a "seepage pattern" would turn into a "driven pattern" under certain conditions. The transition conditions relate to the values of H, D, and d. Figure 4 shows the boundary between the driven and seepage patterns under different test conditions. The size ratio (R_s), defined as D/d_{85}, is usually identified as a single parameter to express the relationship between the grain sizes of porous media and fine particles (Sherard et al. 1984; Wu and Hang et al. 2000), where d_{85} is the size of sand particles at 85% passing. The d_{85} values in the study were 0.2, 0.35, 0.75, and 1.2 mm. The corresponding R_s values ranged from 10 to 125.

The results in Fig. 4 show that the driven pattern easily occurred with an increase in the initial infiltration water head, especially when the value of R_s was higher. However, the probability of the driven pattern was greatly reduced by a decreasing R_s. In this study, the driven pattern was not observed when the R_s value was less than 20. Interestingly, after the infiltration head was below the height of the sand layer, only water flowed through the outlet of the glass beads; few sand particles flowed into the porous medium and most of them were retained by it, possibly because of the strong capillary pressures between sand particles.

Transport Rate

As mentioned earlier, the amount of inrush water and sand from porous media had the characteristics of alternately fluctuating. The characteristics of the instantaneous water flow rate present a certain amount of fluctuation, as shown in Fig. 5. The measurement of $v(t)$ can be made of the change rate of the water level per unit time. To facilitate comparison with different water flow rate results under different conditions, we adopted a time-averaged flow rate ($\overline{v}$) instead of an instantaneous water flow rate. The time average value, which is usually used in the dynamics of streams, is defined as the time integral over the sampling duration (Ballio et al. 2014; Furbish et al. 2017), as shown in Eq. (1).

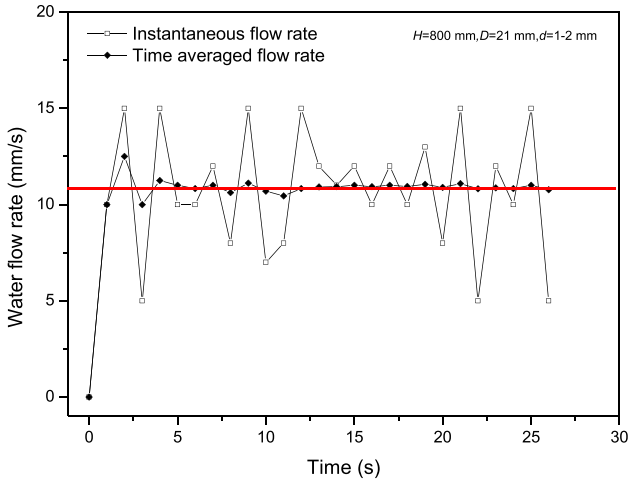

Fig. 5 The instantaneous and time-averaged water flow rate for (H, D, d) = (800, 21, 1–2)

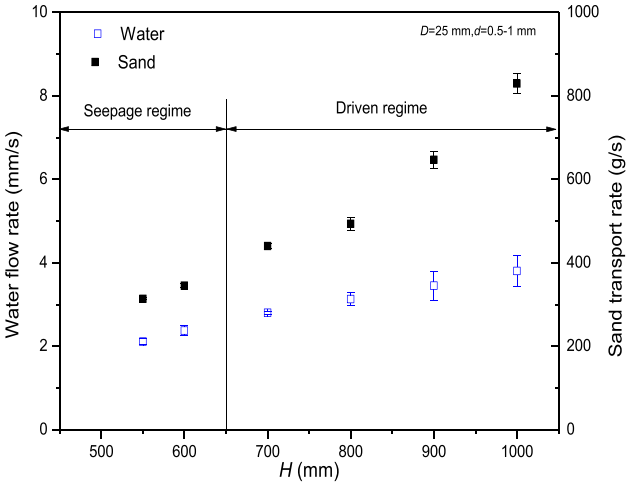

Fig. 6 Variations in the water and sand transport rates under different hydrodynamic conditions for (D, d) = (25, 0. 5–1)

$$\overline{v}_w = \frac{1}{t}\int_{t_0}^{t_0+\Delta t} v_{w,t}dt \tag{1}$$

where $v_{w,t}$ is the instantaneous water flow rate at time t, t_0 is the initial time, and Δt is the sampling duration. The corresponding time-averaged water flow rates are also shown in Fig. 5 and Supplemental Fig. S-2. Note that with increasing sampling duration, the time averaged value ($\overline{v}_w$) tends to a constant value. This result agrees with the conclusion from Ballio et al. (2014) that the time averaged value is a function of the integration time period. Therefore, the time-averaged water flow rates for (H, D, d) = (800, 21, 1–2) and (H, D, d) = (900, 21, 0.25–0.5) were ≈ 10.8 mm/s and 1.5 mm/s, respectively.

Considering that the density of sand during the inrush process is not constant, the time average mass flow rate is used to describe the sand transport rate ($\overline{U}_s$, g/s) at time t, similar to the water flow rate, which can be calculated using Eq. (2).

$$\overline{U}_s = U_{mix} - \overline{U}_w \tag{2}$$

where U_{mix} is the quantity of the discharged mixture of sand and water falling from the porous medium at time t, which can be obtained by scales; $\overline{U}_w$ is the mass of infiltrated water at time t, which can be approximately calculated by using Eq. (3).

$$U_{w,t} = \overline{v}_w \rho_w \mathrm{A}\ (t = 1, 2, \ldots, n) \tag{3}$$

where $v_{w,t}$ is the water flow rate, and the measurement can be made of the change rate of the water level per unit time; ρ_w is the density of water ($\rho_w = 1.0\mathrm{g/cm}^3$), and A is the cross-sectional area of the cylinder.

Transport Rate under Different Hydraulic Conditions

A series of experiments was performed to characterize the influence of the initial infiltration water head (H) on the water and sand transport rates (Fig. 6). As expected, both the water flow and sand transport rates increased with increasing initial infiltration heads. Furthermore, the increase in the initial infiltration head increased the magnitude of the sand transport rate much more than it increased the water flow rate. For example, when the initial infiltration heads increased from 550 to 1000 mm, the sand transport rate for (D, d) = (25 mm, 0.5–1 mm) sharply increased from 314.0 g/s to 829.8 g/s, and the corresponding water flow rate only increased from 2.11 mm/s to 3.81 mm/s. Similar observations were made under the condition of (D, d) = (21 mm, 0.25–0.5 mm), as shown in Supplemental Fig. S-3. For example, when H increased from 550 to 1000 mm, the sand transport rate increased from 78.6 g/s to 427.9 g/s, and the water flow rate only increased from 0.82 mm/s to 1.68 mm/s. Therefore, the infiltration water head had a greater influence on the sand transport rate than the water flow rate.

Transport Rate at Different Size Ratios

To investigate the effects of the size of materials used in the investigation on the water and sand transport rate, the experiments were carried out with four different sand grains (d) under three different porous media packed with different glass beads (D). The results are shown in Fig. 7. Note that the higher the water head was, the larger the water flow and sand transport rates. Figure 7a shows the influence of R_s on the water flow rate. The water flow rate of the sand layer with a larger grain size was greater than in a sand layer with a smaller grain size. When the water head, H = 600 mm, the

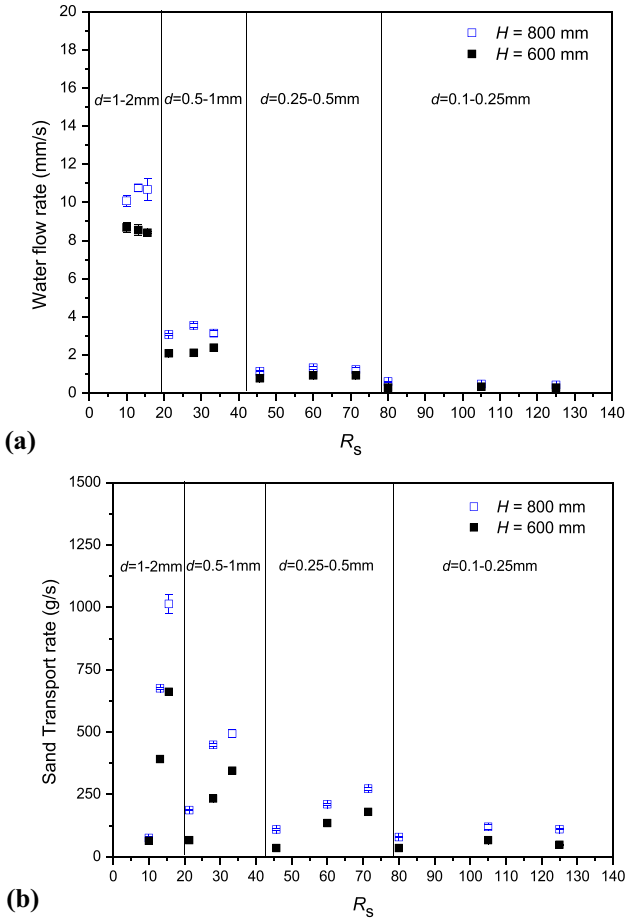

Fig. 7 The influence of R_s on the **a** water flow rate and **b** sand transport rate

water flow rate for $d = 1$–22 mm was ≈ 8.5 mm/s, whereas the water flow rate for $d = 0.1$–0.25 mm was 0.3 mm/s. Nevertheless, there was only a slight difference in the water flow rate for the same sand particle size (d). The water flow rate was primarily governed by the size of the sand particles, which can be explained by the fact that the permeability of the sand layer usually increases with increasing sand particle size. Thus, the larger the sand particles are, the higher the water flow rate.

However, the influences of R_s (which depends entirely on D for the same sand layer) on the sand transport rate for different sand particles vary widely (Fig. 7b). When the sand particle size $d = 0.1$–0.25 mm, there was no significant difference in the sand transport rate of ≈ 100 g/s. For other sand particles, such as $d = 0.25$–0.5 mm, 0.5–11 mm, and 1–22 mm, the sand transport rate increases with increasing R_s. Furthermore, the rate of increase of the sand transport rate was greater for larger sand particles. Taking the condition of $H = 600$ mm as an example, when D ranged from 16 to 25 mm, the sand transport rate with $d = 0.25$–0.5 mm varied from 34 g/s to 179 g/s, whereas those with the transport rate $d = 1$–22 mm only increased from 63 g/s to 661 g/s. Therefore, the influence of R_s on the sand transport rate was gradually stronger with increasingly large particles. A significant change in the sand transport rate was also observed for $H = 800$ mm.

Figures 7a and 7b show that a large sand transport rate and low water flow rate are the main flow characteristics of sand/water mixture inrushes. This is consistent with field observations of sand/mud/water inrush disasters: large amounts of sand, small amounts of water, and low permeability coefficients (Miao et al. 2010).

Discussions

Water Flow Rate

Darcy's law is not appropriate for the sand/mud/water mixture inrush process, since the two-phase flow is usually regarded as turbulent flow. However, the mixed inrush may be regarded as a filtration process, with the inference that the water flow rate (v_w) during the inrush would increase with greater coefficients of permeability (k) and water head loss (Δh), but would decrease with sample distance (L).

The coefficient of permeability for coarse to fine sand is about 10^{-1} to 10^{-3} cm/s, which is far less than that of the porous medium. Hence, the water flow rate during the inrush process is governed mainly by the sand layer instead of the porous medium. Once the values of d and D are determined, the coefficient of permeability (k) will be slightly changed. The water flow rate (v_w) is affected by the hydraulic head difference between both ends of the sample. In general, the greater the initial hydraulic head, the greater the hydraulic head difference. This is why the water flow rate (v_w) increases with increasing initial hydraulic head. In addition, the water flow rate (v_w) depends mainly on the coefficient of permeability (k) of the sand at the same initial hydraulic conditions, which explains why the water flow rate does not increase with increasing R_s for the same sand particle.

Sand Transport Rate

The transport of particles in porous media has significant implications in a variety of disciplines and has received considerable attention (e.g. Ahfir et al. 2017; Locke 2001; Reddi 1997). Most previous studies have investigated the transport of suspended particles through porous medium, and revealed that along with hydrodynamic conditions, fine particle size, pore size, and pore distribution in porous media are the main controlling factors (Ahfir et al. 2007; Benamar et al. 2007; Imdakm and Sahimi 1987). This conclusion is consistent with our experimental data. However, for suspended particles (a size of 0.1–10 μm), all forces and mechanisms can

contribute to particle transport (Ahfir et al. 2007; Pinheiro et al. 1999), while for particles exceeding 100 µm in size, and at higher water head, the forces are quite different. When water percolates through the sand layer, water exerts seepage pressure (J) on the sand particles, which is defined as:

$$J = \frac{\Delta H}{L}\gamma_w \tag{4}$$

In principle, a higher initial water head, which produces a higher hydraulic pressure and enhances seepage pressure, should accelerate the sand transport rate. However, the permeation of water through the sand layer also decreases the water head, which gradually reduces the seepage pressure and decreases the sand transport rate.

In addition, the effect of filtration and clogging cannot be ignored as the sand particles flow through porous media, which depends mainly on the size of the sand particles and porous media pores. When the sand particles are small, they can easily migrate through a porous medium, so the sand transport rate is affected mainly by the size of sand particles. When the sand particles are large, the sand transport rate is gradually governed more by the voids in the porous media because the probability of sand particles being captured significantly increases as the number of sand particles increases. For smaller R_s values (i.e. for $d = 1$–2 mm and $D = 16$ mm, $R_s = 10$), the probability of sand particle deposition significantly increases, which greatly reduces the sand transport rate. As the size ratio R_s increases, a larger portion of input sand particles penetrate through the porous media without being trapped by the solid structure.

The two types of flow patterns, seepage and driven, are mainly dependent on the water and sand transport rates. The water flow rate is controlled mainly by the permeability of the sand layer and initial water head. The sand flow rate is mainly influenced by the seepage pressure on the sand layer and the size ratio R_s. Given that the permeation of water through the sand layer decreases the water head height, the higher the permeability of the sand layer, the greater the water flow rate, which in turn facilitates the dissipation of hydraulic potential and seepage pressure on the sand layer. When the water surface fell below the top of the sand layer, seepage pressure disappeared as capillary pressure gradual developed, and became the dominant force between the soil particles, eventually stopping sand transport. In contrast, when the permeability of the sand layer is low, the water flow rate is low, which prolongs the flow process. That is the main reason why, in the driven pattern, the sand layer was depleted before all of the water had left.

Clogging

Clogging is important to prevent the sand/mud/water mixture flow inrush. At low water flow rates, the deposition and accumulation of fine sand particles can block the voids and pores in the caving zone, and help prevent sand/mud/water mixture inrushes. For example, Zhang and Hou (2005) found that despite surface subsidence on the ground surface, there was no water and sand inrush into the panels in the Daliuta Coal Mine. This indicated a clogging of sand above or in the caving zone. The seepage pattern in this study can be regarded as one kind of clogging. After the water had entirely drained, the sand in the cylinder column still maintained a certain height. Figure 8 shows a photo and schematic of the seepage pattern after a test. Note that the sand particles are not only deposited inside the porous media, but also at the surface above the porous medium. These phenomena are respectively referred to as internal and external filter cakes.

Fine particles with a size equal to or larger than the size of porous medium ($R_s \leq 1$) will be trapped at the surface above the porous medium and form an external filter cake. An internal filter cake formed when R_s ranged from 4 to 15 (Jung et al. 2018; Kerimov et al. 2018; Racha Medjda et al. 2020). The R_s obtained in this study was much higher than reported in previous studies. A seepage pattern can form when R_s is less than 20, and even greater than that at lower water flow rates. The different values of R_s in previous studies are attributed to the low suspended solid particle concentrations (about 15 to 30%) (Agbangla et al. 2012; Jung et al. 2018; Valdes et al. 2008), while in this study, the concentration of sand particles reached 90%, which greatly increased the value of R_s.

In practice, pore geometry and distribution would greatly influence the likelihood of blockage of the caving zone during a sand inrush (Benamar et al. 2007; Neuman and Tartakovsky 2009; Tartakovsky and Dentz 2019). Glass beads with the same size lead to a uniform pore distribution, which

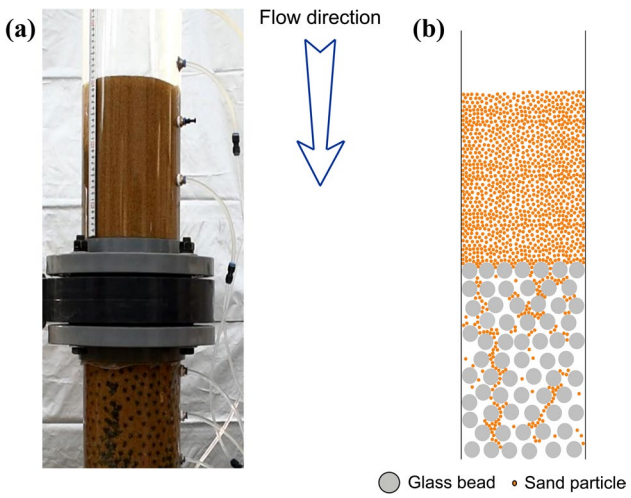

Fig. 8 The **a** photo and **b** schematic of seepage pattern after test

facilitates sand particle transport. However, in real life, the caving zone is not completely porous media and there exists many disconnected and dead-end pores that can restrain the movement of sand particles. The geometry of dead-end pores is like a stagnant pocket and deposition and accumulation of sand particles is more likely in these zones (Biswas and Kartha 2019). Thus, sand particles can only migrate through well interconnected pores, likely leading to preferential flow (Liang et al. 2017). Indeed, caving zones do, to some extent, block inrushes of sand/mud/water mixtures.

Implications for Control of Sand/Mud/Water Mixtures

As mentioned earlier, clogging plays an important role in preventing inrushes of sand/mud/water mixtures in the caving zone. Therefore, it is important to take measures to increase the probability of clogging. Obviously, reducing the initial infiltration water level in an unconsolidated layer is an effective option, but the results from this study also indicate that the reducing the size ratio R_s will greatly increase the likelihood of blockage during a sand inrush into caving zone. In some cases, rock aggregates or sands could be pumped into a caving zone or subsided pit to control inrushes of sand/mud/water mixtures into the mining panel.

Limitations

As granular flow shows a rich variety of rather astonishing and scarcely understood phenomena, modeling granular flows is very difficult. For example, alternating fluctuations occurred as the sand/mud/water mixture flowed through the porous media. Similar behavior has been reported in granular dynamics research, and has been called a density wave (Raafat et al. 1996; Reydellet et al. 2000). Although the mechanism of this behavior has not been identified, this fluctuating would certainly greatly affect flow through pathways similar to caving zones, such as fractures or collapsed karst pillars. This will be the focus of our future research.

The experimental work in this study was not intended to simulate any mine site, and the experimental design does not strictly follow the similarity law. For example, to simplify the problem of caving zones with water and sand flows, an ideal porous medium was used in this study to demonstrate the simple case of a caving zone full of broken rock. Furthermore, we focused mainly on transport propagation in the caving zone in this study and did not measure variations in the height of the sand layer, which we will consider in the future.

Clay content also influences the transport behavior of solid-water mixtures. The location, content, and composition of clay particles in unconsolidated layers would affect the transport characteristics of a sand/mud/ water mixture during an inrush. Xu (2008) found that the movement of sand/mud/water mixtures was decreased by greater clay content in medium sand, but had only a slight effect on fine sand mixtures. In contrast, Chen et al. (2021) showed that both 5% and 10% clay content promoted the occurrence of sand/mud/water inrushes. To reduce uncertainties that would have considerably complicated the analysis of experimental data, the influence of clay content was not considered in this study. In addition, chemical reactions between the mine water and the soil's mineral components may also have influenced the transport behavior; the combination of these factors should be investigated in the future.

Conclusions

To better understand the transport behavior of sand/mud/water mixtures in the caving zone, we performed a series of experiments under a variety of conditions in this study. The following were the main conclusions:

(1) We observed two transport patterns, a seepage pattern and a driven pattern, during experimental observations of the transport behavior of sand/mud/water mixtures in porous media. The change from a seepage pattern to a driven pattern depended on the initial height of the water head and size ratio, R_s. Generally, the driven pattern was more likely with a greater initial infiltration water head, especially when the value of R_s was higher. The driven pattern is not observed once the size ratio R_s was less than 20 in this study.
(2) The sand and water transport rate were described using a time-averaged rate due to the alternating fluctuating behavior of the sand/mud/water mixture. In general, the sand transport rate was greater than the water flow rate. An increase of the initial water head increased both transport rates, but the increase in the sand transport rate was much larger. In addition, for the same initial water level, the water flow rate was primarily governed by the permeability of the sand layer. The water flow rate was greatly reduced by the decreasing permeability of the sand layer. As the value of R_s decreased, the likelihood of sand particles depositing and clogging the pores of the porous medium increased, which greatly reduced the sand transport rate. The influence of R_s on the sand transport flow rate was more obvious with larger sand particles.
(3) The occurrence and severity of sand/mud/water mixture inrushes mainly depend on the initial height of the water head and size ratio, R_s. Therefore, reducing the in-situ water level in an unconsolidated layer and the R_s value of the caving zone, by pumping rock aggregate or

larger diameter sand particles into the fractured zone or caving zone, would greatly decrease the likelihood of sand/mud/water mixture inrush disasters.

Supplementary Information The online version contains supplementary material available at https://doi.org/10.1007/s10230-022-00852-z.

Acknowledgements The authors acknowledge financial support from the National Natural Science Foundation of China under Grant 41902283 and 42130706. The authors thank Shichong Yuan and Jiahao Wang of the China University of Mining and Technology for their assistance with the testing.

Funding This work was supported by National Natural Science Foundation of China (Grant Nos. 42130706 and 41902283).

References

Agbangla GC, Climent É, Bacchin P (2012) Experimental investigation of pore clogging by microparticles: evidence for a critical flux density of particle yielding arches and deposits. Sep Purif Technol 101:42–48

Ahfir ND, Wang HQ, Benamar A, Alem A, Massei N, Dupont JJ (2007) Transport and deposition of suspended particles in saturated porous media: hydrodynamic effect. Hydrogeol J 15(4):659–668

Ahfir ND, Hammadi A, Alem A, Wang HQ, Bras GL, Ouahbi T (2017) Porous media grain size distribution and hydrodynamic forces effects on transport and deposition of suspended particles. J Environ Sci 53:161–172. https://doi.org/10.1016/j.jes.2016.01.032

Ballio F, Nikora V, Coleman SE (2014) On the definition of solid discharge in hydro-environment research and applications. J Hydraul Res 52(2):173–184. https://doi.org/10.1080/00221686.2013.869267

Benamar A, Ahfir ND, Wang H, Alem A (2007) Particle transport in a saturated porous medium: pore structure effects. CR Geosci 339(10):674–681

Biswas D, Kartha SA (2019) Conceptual modeling of temperature effects on capillary pressure in dead-end pores. Sādhanā 44(5):1–12. https://doi.org/10.1007/s12046-019-1108-y

Butcher R, Stacey TR, Joughin WC (2005) Mud rushes and methods of combating them. J South Afr Inst Min Metall 105(11):817

Campbell CS (2006) Granular material flows–an overview. Powder Technol 162(3):208–229

Chen ZQ, Yu BY (2015) Research progress of seepage mechanics in rock mass affected by mining. J SW Petrol Univ Sci Tech 37(3):69–76 ((**in Chinese**))

Chen LW, Zhang SL, Gui HR (2014) Prevention of water and quicksand inrush during extracting contiguous coal seams under the lowermost aquifer in the unconsolidated Cenozoic alluvium-a case study. Arab J Geosci 7:2139–2149. https://doi.org/10.1007/s12517-013-1029-8

Chen JR, Pu H, Xiao C, Liu GH (2016) Experimental study of impact of deformation history on water-sand seepage characteristics of broken rock. J Min Safe Eng 33(2):329–335 ((**in Chinese**))

Chen B, Zhang SC, Li YY, Li JP (2021) Experimental study on water and sand mixture inrush of mining cracks in loose layers with different clay contents. Bull Eng Geol Environ 80:663–678. https://doi.org/10.1007/s10064-020-01941-5

China Central Television (2021) Water and sand mixture inrush hazard occurred in Haojialiang coal mine in Yulin Shanxi. https://news.cctv.com/2021/07/16/ARTIZ3hTbE9ULARMERFHt52o210716.shtml. Accessed 19 Jul 2021

Cochard S, Ancey C (2009) Experimental investigation of the spreading of viscoplastic fluids on inclined planes. J Nonnewton Fluid Mech 158(1):73–84. https://doi.org/10.1016/j.jnnfm.2008.08.007

Dept. of Emergency Management of Shaanxi Province (2021) Report of 7.15 water and sand disaster in Haojialiang coal mine, Yulin. https://www.163.com/dy/article/GFCO0BUK0538N2MQ.html Accessed 20 Jul 2021

Dong SN, Ji YD, Wang H, Zhao BF, Cao HD, Liu Y, Liu YF, Ji ZK, Liu BG (2020) Prevention and control technology and application of roof water disaster in Jurassic coal field of Ordos Basin. J Chin Coal Soc 45(7):2367–2375 ((**in Chinese**))

Du F, Li ZH, Jiang GH, Chen ZQ (2017) Types and mechanism of water-sand inrush disaster in west coal mine. J Chin Coal Soc 42(7):1846–1853 ((**in Chinese**))

Du F, Cao ZZ, Li ZH (2018a) Research progress of two-phase water-sand flow characteristics in crushed rock mass. Coal Sci Technol 46(7):48–53 ((**in Chinese**))

Du F, Jiang GH, Chen ZQ (2018b) A numerical simulation study of the migration law of water-sand two-phase flow in broken rock mass. Geofluids 2018:1–12. https://doi.org/10.1155/2018/6418476

Forterre Y, Pouliquen O (2008) Flows of dense granular media. Annu Rev Fluid Mech 40:1–24

Furbish DJ, Fathel SL, Schmeeckle MW, Jerolmack DJ, Schumer R (2017) The elements and richness of particle diffusion during sediment transport at small timescales. Earth Surf Process Landf 42(1):214–237

Goldhirsch I (2003) Rapid granular flows. Annu Rev Fluid Mech 35(1):267–293

Guo WJ, Wang HL, Chen SJ, Li JP (2016) Development and application of simulation test system for water and sand mixture inrush across overburden fissures due to coal mining. Chin J Rock Mech Eng 35(7):1415–1422 ((**in Chinese**))

Haza ZF, Harahap ISH, Dakssa LM (2013) Experimental studies of the flow-front and drag forces exerted by subaqueous mudflow on inclined base. Nat Hazards. https://doi.org/10.1007/s11069013-0643-9

Imdakm AO, Sahimi M (1987) Transport of large particles in flow through porous media. Phys Rev A 36(11):5304

Jung J, Cao SC, Shin YH, Al-Raoush RI, Alshibli K, Choi JW (2018) A microfluidic pore model to study the migration of fine particles in single-phase and multi-phase flows in porous media. Microsyst Technol 24(2):1071–1080. https://doi.org/10.1007/s00542-017-3462-1

Kerimov A, Mavko G, Mukerji T, Ibrahim MA (2018) Mechanical trapping of particles in granular media. Phys Rev E 97(2):022907

Li Z, Sui WH, Zhang XJ (2016) Experimental investigation on movement and stress fluctuation of quicksand inside fissure. J Eng Geol 24(5):981–991 ((**in Chinese**))

Liang YK, Sui WH, Zhu T, Zhang XJ (2017) Numerical simulation of quicksand through the broken rocks in caving zone due to coal mining based on DEM. J Chin Coal Soc 42(2):470–476 ((**in Chinese**))

Liu Y, Li SC (2016) Influence of particle size on non-Darcy seepage of water and sediment in fractured rock. Springerplus 5(1):2099. https://doi.org/10.1186/s40064-016-3778-9

Locke M, Indraratna B, Adikari G (2001) Time-dependent particle transport through granular filters. J Geotech Geoenviron 127(6):521–529

Miao XX, Wang CS, Bai HB (2010) Hydrogeologic characteristics of mine water hazards in the Shendong mining area. J Min Safe Eng 27(3):285–291 (**in Chinese**)

Neuman SP, Tartakovsky DM (2009) Perspective on theories of non-Fickian transport in heterogeneous media. Adv Water Resour 32(5):670–680

Pinheiro IG, Schmitz P, Houi D (1999) Particle capture in porous media when physico-chemical effects dominate. Chem Eng Sci 54(17):3801–3813

Qian QH (2012) Challenges faced by underground projects construction safety and countermeasures. Chin J Rock Mech Eng 31(10):1945–1956 ((**in Chinese**))

Qian ZW, Jiang ZQ, Guan YZ, Yue N (2019) Mechanism and remediation of water and sand mixture inrush induced in an inclined shaft by large-tonnage vehicles. Mine Water Environ 37:849–855. https://doi.org/10.1007/s10230-018-0531-3

Raafat T, Hulin JP, Herrmann HJ (1996) Density waves in dry granular media falling through a vertical pipe. Phys Rev E 53(5):4345

Racha Medjda BK, Abdelghani CF, Maxime P, Zohra GF (2020) The trapping of colloid particles in porous media: mechanisms and applications, review. J Appl Res Water Wastewater 7(2):180–188

Reddi LN (1997) Particle transport in soils: review of significant processes in infrastructure systems. J Infrastruct Syst 3(2):78–86

Reydellet G, Rioual F, Clement E (2000) Granular hydrodynamics and density wave regimes in a vertical chute experiment. Europhys Lett 51(1):27

Sherard JL, Dunnigan LP, Talbot JR (1984) Basic properties of sand and gravel filters. J Geotech Eng 110(6):684–700

Sui WH, Cai GT, Dong QH (2007) Experimental research on critical percolation gradient of quicksand across overburden fissures due to coal mining near unconsolidated soil layers. Chin J Rock Mech Eng 26(10):2084–2091 ((**in Chinese**))

Sui WH, Dong QH, Cai GT, Yang WF, Hang Y (2008) Quicksand hazards in underground coal mines: mechanism and prevention. Geological Publishing House, Beijing (**in Chinese**)

Sui WH, Liang YK, Zhang GL, Dong QH, Yang BB (2011) Study status and outlook of risk evaluation on water inrush and sand inrush mechanism of excavation and mining. Coal Sci Technol 39(11):5–9 ((**in Chinese**))

Sui WH, Liang YK, Zhang XJ, Ravi J, Zhu T (2017) An experimental investigation on the speed of sand flow through a fixed porous bed. Sci Rep 7(54):1–8. https://doi.org/10.1038/s41598-017-00082-2

Tartakovsky DM, Dentz M (2019) Diffusion in porous media: phenomena and mechanisms. Transport Porous Med 130(1):105–127

Valdes JR, Santamarina JC (2008) Clogging: bridge formation and vibration-based destabilization. Can Geotech J 45(2):177–184

Wu FC, Huang HT (2000) Hydraulic resistance induced by deposition of sediment in porous medium. J Hydraul Eng 126(7):547–551

Xu YC (2008) Fluidity test on sand blended with clay. J Chin Coal Soc 33(5):496–499 ((**in Chinese**))

Xue YG, Kong FM, Li SC, Qiu DH, Su MX, Li ZQ (2021) Water and mud inrush hazard in underground engineering: genesis, evolution and prevention. Tunn Undergr Sp Tech 114:103987. https://doi.org/10.1016/j.tust.2021.103987

Yang X, Xu ZH, Yang TH, Yang B, Shi WH (2018) Incipience criterion and migration character of aeolian-sand aquifer water-sand inrush in typical western mine. Rock Soil Mech 39(1):1–9 ((**in Chinese**))

Yang B, Yang TH, Xu ZH, Liu HL, Yang X, Shi WH (2019a) Impact of particle-size distribution on flow properties of a packed column. J Hydrol Eng 24(3):04018070

Yang WF, Jin L, Zhang XQ (2019b) Simulation test on mixed water and sand mixture inrush disaster induced by mining under the thin bedrock. J Loss Prev Process Ind 57:1–6. https://doi.org/10.1016/j.jlp.2018.11.007

Yang X, Liu YJ, Xue M, Yang TH, Yang B (2020) Experimental investigation of water–sand mixed fluid initiation and migration in porous skeleton during water and sand mixture inrush. Geofluids 2020(12):1–18. https://doi.org/10.1155/2020/8679861

Zhang J, Hou ZJ (2005) Study on sand inrush disaster in shallow seam mining. J Hunan U Sci Tech Nat Sci 20(3):15–18 (**in Chinese**)

Zhang GM, Zhang K, Wang LJ (2015) Mechanism of water inrush and quicksand movement induced by a borehole and measures for prevention and remediation. B Eng Geol Environ 74(4):1395–1405. https://doi.org/10.1007/s10064-014-0714-5

Zhang C, Zhao YX, Tu SH, Zhang T (2020) Numerical simulation of compaction and re-breakage characteristics of coal and rock samples in goaf. Chin J Geotech Eng 42(4):696–704 (**in Chinese**)

Zhang BY, He QY, Lin ZB, Li ZH (2021) Experimental study on the flow behaviour of water-sand mixtures in fractured rock specimens. Int J Min Sci Technol 31(3):377–385. https://doi.org/10.1016/j.ijmst.2020.09.001

Zhao Y, Li P, Tian S (2013) Prevention and treatment technologies of railway tunnel water inrush and mud gushing in China. J Rock Mech Geotech Eng 5(6):468–477. https://doi.org/10.1016/j.jrmge.2013.07.009